Proceedings World Geothermal Congress 2020+1
Reykjavik, Iceland, April - October 2021

Investigation of Non-Ionic Polymer as a Suitable Inhibitor in Protecting Carbon Steel from the Aggressive Corrosion of Acidic Simulated Geothermal Brine

Jennifer Espartero-Dales[1], Al Christopher de Leon[2], and Rigoberto Advincula[2]

[1]Energy Development Corporation, Southern Negros Geothermal Production Field, Ticala, Valencia, Philippines

[2] Department of Macromolecular Science and Engineering, Case Western Reserve University, Cleveland, Ohio, USA

espartero.jc@energy.com.ph

Keywords: silica, corrosion inhibitor, acidic geothermal brine

ABSTRACT

The use of inhibitors is considered to be one of the most economical and practical corrosion technology solutions. However, this technology is still underutilized in EDC geothermal fields due to the complexity of the geothermal brine which makes it difficult to find a compatible inhibitor available in the market. A good geothermal corrosion inhibitor should be able to control the corrosion rate at an acceptable level without causing any significant change to the brine chemistry that could lead to unwanted mineral scaling. Other factors that need to be considered in the selection of inhibitors are thermal stability, good solubility even at high ionic concentrations, and a wide pH range.

For this study, we used a nonionic water-soluble polymer reported to be a good cathodic inhibitor and at the same time can promote silica layer formation. Despite the abundance of silica in geothermal brine, it is not easily deposited in low pH conditions since it is present in solution as silicic acid, which is very soluble in the brine and tends to be well dissolved in solutions. If the polymer can promote silica deposition, it could act not only as a corrosion inhibitor but can also add as an additional barrier from the corrosive species present in the brine.

Various characterization techniques such as Scanning Electron Microscopy (SEM), X-ray Photoelectron Spectroscopy (XPS), and Fourier Transform-Infrared (FT-IR) were done to determine inhibition mechanism of the polymer to carbon steel immersed in simulated acidic geothermal brine. The anti-corrosion property of the inhibitor was further tested using the weight loss method, Electrochemical impedance spectroscopy (EIS), potentiodynamic polarization scan (PPS), and open-circuit potential measurements (OCP). The mechanism of corrosion inhibition action of the polymeric inhibitor is proposed based on the results of the analysis made throughout the course of the study.

1. INTRODUCTION

The use of polymers as effective inhibitors is a popular option for corrosion control. Its use, however, in geothermal industries is limited by the complexity of the geothermal brine. A good geothermal corrosion inhibitor should be able to control the corrosion rate at an acceptable level without causing any significant change to the brine chemistry that could lead to unwanted mineral scaling. Another factor to consider is the thermal stability of the inhibitor to be used since the process temperature of a geothermal system is between 160-350°C. In addition, inhibiting agents are effective only if their solubility in the corrosive environment is optimal. Very low solubility of inhibitor leads to lack of active agent at the metal interface and consequently to weak inhibition. If the solubility is too high, the substrate will be protected, but only for a relatively short time since the inhibitor will be rapidly leached out from the coating based on the study conducted by El-Maksuod (2008). Due to the dissolved minerals in any given geothermal brine, its ionic strength is high. This would limit the use of polymers that are not stable at high ionic medium. Instead of dissolving, they precipitate out from the solution. Because the pH of each geothermal well is different, the use of pH sensitive polymers may also not be suitable for the application. The pH range at which the inhibitor is soluble should be broad so that it has a wide scope of application and for it to be economical and practical. Based on the observations made by Thomas (2008), Zheludkevich et al. (2007), and Umoren et al. (2008), a good corrosion inhibitor should satisfy the following requirements: a) it should easily oxidize the metal surface to form an impervious and compact film; b) it should have highly disposable sites for chemisorption to take place onto the metal surface; c) the barrier film must be able to cover a large area of the metal surface; d) it should be polymeric in nature or be able to polymerize on the surface of the metal; and, e) eco-friendly, low cost, safe in handling, and readily available.

Based on the evaluation conducted, a non-ionic polymer (NIP) was selected which possess the recommended properties as a suitable corrosion inhibitor in acidic geothermal system. NIP has attracted great attention in the field of colloid and interface science because it was found that various stable oxide or metal colloids could be attained with the addition of NIP. It exhibits mesomeric structures which make it possible for its molecules to form hydrogen bond or coordination linkage with various oxides or metals (Fe, Mn, Co, Zn, and Ni). NIP has also been reported to promote deposition of silica. It is widely reported that films formed by silica are good anti-corrosion coating. Despite the abundance of silica in geothermal brine, it is not easily deposited in low pH conditions since it is present in acidic solution as silicic acid, which is very soluble in the brine and tends to be well dissolved in solutions. If the deposition of silica could be promoted by NIP, it could act not only as a corrosion inhibitor but can also add as an additional barrier from the corrosive species present in the brine.

2. MATERIALS AND METHODOLOGY

NIP purchased from Aldrich chemicals with varying molecular weights (10K, 40K, and 360K) were used as received.

2.1. Substrate preparation

The carbon steel (CS) sheets were first cut into1.5 x 2.0 cm pieces and were prepared according to the ASTM G1 standard. They were then sonicated in acetone for 15-20 min, dried, and kept under vacuum prior to use.

2.2 Immersion study

Polished CS were immersed in 100 ml of simulated geothermal brine in a plastic container with cover at varying MW (10K, 40K,and 360K), varying concentrations (5 ppm, 10 ppm, and 15 ppm), varying duration (2 days, 7 days, 14 days, 30 days, and 60 days), and varying temperature (25°C and 180°C).

2.3 Instrumentation

The FT-IR spectroscopy was done with FTIR Spectrometer and scanned between 4000 and 400 cm^{-1}. All spectra were recorded with nominal spectral resolution of 2 cm^{-1} and 128 scans were collected and averaged for each spectrum.

Electrochemical measurements for the evaluation of anti-corrosion property were done using a Potentiostat, with platinum as the counter electrode, Ag/Ag+ in 0.5 M NaCl as the reference electrode, and the carbon steel substrates as the working electrodes. Potentiodynamic polarization scan (PPS) was performed by scanning from −0.025 to +0.025 V vs Ag/Ag+ reference electrode (0.5 M NaCl) about the open circuit potential (OCP) while electrochemical impedance spectroscopy (EIS) was performed for seven frequency decades from 10 mHz to 100 kHz with an amplitude of 10 mV with respect to the OCP.

3. RESULTS AND DISCUSSION

3.1 Selection of concentrations to be tested

One requirement of a good inhibitor is its good solubility in the corrosive solution, which in this case is the acidic geothermal brine. Since there was no reported study on the use of NIP as corrosion inhibitor in geothermal industries, a simple solubility test was conducted to determine the range of inhibitor concentration to be tested. NIP solutions with concentration ranging from 10-1000 ppm were prepared for the solubility test as shown in Figure 1. The concept of Tyndall effect was applied to determine the maximum amount of NIP where it is still soluble in the desired medium. The Tyndall effect is usually given as a definitive test to distinguish between a true solution and a colloid. It involves the scattering of a beam of light as the light passes through a medium having particles of colloidal size. Figure 1 shows the result of the Tyndall effect to solutions of increasing concentration of NIP in the geothermal brine. Based from the test conducted, NIP has an acceptable solubility at 50 ppm. However, due to economic concerns, it is desired that the optimum concentration of inhibitors should be as low as possible to lessen the cost of the inhibition system. Reducing the concentration of inhibitor in half would translate to half the cost as well of the inhibitors to be used, earning significant savings. For this study, concentration of 5, 10, and 15 ppm NIP were chosen to be tested and evaluated.

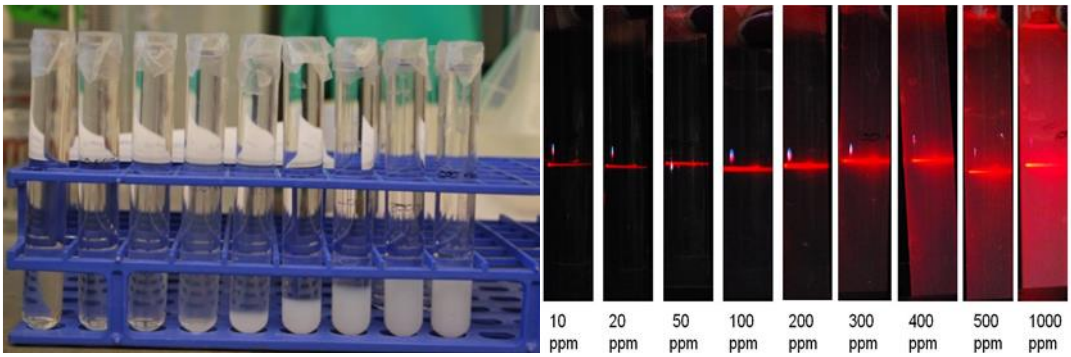

Figure 1: Varying concentration NIP (10, 20, 50, 100, 200, 300, 400, 500, and 1000 ppm) for solubility testing and the corresponding result of the Tyndall effect test.

3.2 Evaluating the effect of MW of NIP in corrosion inhibition

To determine the optimum concentration of NIP, varying MW of NIP were tested using Electrochemical Impedance Spectroscopy (EIS) and Potentiodynamic Polarization Scan (PPS) tests. The inhibition efficiency (IE) of the CS immersed for one month in varying MW of NIP was determined using the Tafel analysis. This is done by varying the potential about the OCP and plotting the logarithm of the resulting current against the applied potential. Corrosion currents (Icorr) and corrosion potentials (Ecorr) were then determined by numerically fitting the resulting Tafel plots to the Butler-Volmer Equation. Icorr and Ecorr are extracted via a computer routine by specifying the cathodic and anodic branches and using non-linear least square fitting method of Levenberg/Marquardt. The inhibition efficiency is calculated using the equation:

$$IE = \left(\frac{I_{corr,bare} - I_{corr,coated}}{I_{corr,bare}}\right) \times 100\% \quad (1)$$

Studies suggest that MW of polymeric inhibitors can have an effect on the inhibition properties due to the repulsive lateral interactions between neighboring molecules or steric effects that could hinder the adsorption of films. A low (10K), mid (40K), and high (360K) MW of NIP were tested to determine the most suitable MW of NIP for an acidic geothermal system. Figure 2 presents inhibition efficiencies of varying MW and concentrations of NIP immersed in acidic geothermal brine for one month.

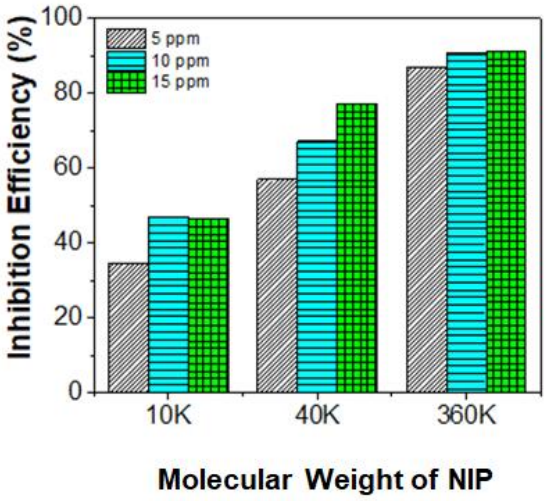

Figure 2: Inhibition efficiencies of varying MW and concentration of NIP in brine solution.

Results show that there is a significant increase of corrosion protection efficiency as the MW of NIP increases. This trend was also observed on the increasing concentration of NIP in acidic geothermal brine solution. Carbon steel immersed in 15 ppm of 360K NIP yields the highest corrosion protection efficiency of 91.33%. This could be attributed to the formation of silica film on the adsorbed NIP on carbon steel. It has been reported that NIP has proven to promote silica film formation on iron nanoparticles in sol-gel system.

FT-IR spectra were obtained to determine the effect of MW by comparing the amount of silica film formed on the surface by examining the stretching of Si-O bond at 1068 cm^{-1}. As observed in Figure 3, there is a direct relationship between the increasing MW and the silica found on the surface of the immersed carbon steel. Higher amounts of NIP in solution would increase the quantity of NIP formed, while higher MW would ensure more coverage of the film form on the metal surface. This trend was observed in the study conducted by Al Juhaiman et al. (2012), where the degree of protection increased with increasing NIP concentration due to the higher degree of surface coverage, which resulted from enhanced inhibitor adsorption. Steric hindrance only begins to dominate in the solution when the highest concentration of NIP is reached based on the study conducted by Daouadji and Chelali (2003). Since the immersion study done was in a static condition, there was no additional amount of NIP was added to the solution. This observation, however, may stand true when the study is to be conducted at flowing conditions. A separate evaluation must be conducted since increased concentration of the polymer would also lead to an increase in the viscosity which would make the transfer of polymer chains from the solution to the metal surface become more difficult.

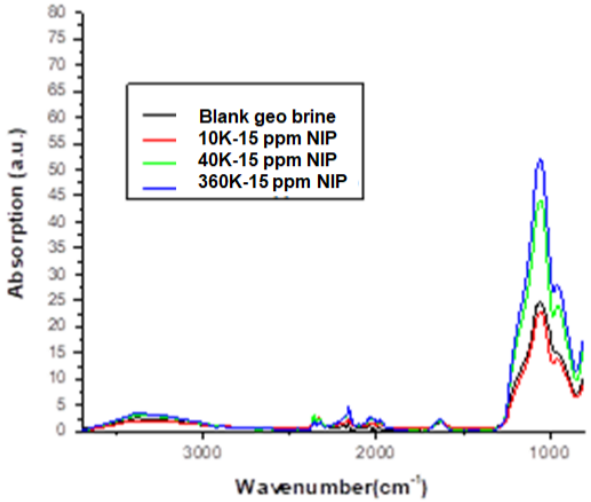

Figure 3: FT-IR spectra of increasing MW of NIP relating to its effect on the effect on the amount of silica formed at 1068 cm^{-1}.

Another important data that could be derived from the FTIR spectra is the interaction of the NIP to the surface metal. As discussed by Salehi et al. (2011), NIP has a carboxyl group characteristic absorption at 1660 cm^{-1} and a carbon-nitrogen adsorption at 1290 cm^{-1}. The presence of a peak at 1293 cm-1, shown in Figure 4, of all samples immersed with NIP, and none with the blank, suggests that NIP is present at the CS surface. It is also apparent that as the MW of NIP increases, the intensity of the absorbance also increases, which supports the result of the previous discussion.

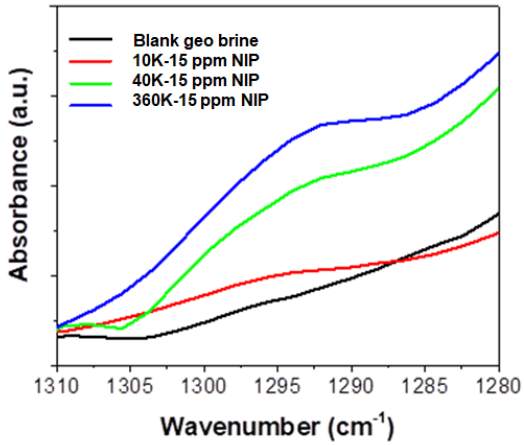

Figure 4: FT-IR spectra of increasing NIP relating to its effect on the carbon-nitrogen adsorption at 1290 cm^{-1}.

It was also observed that there is a shift of the C=O absorption band of NIP from 1660 to 1630 cm^{-1} as shown in Figure 5. The shift, as reported by Qiu et al. (2014), was due to the interaction of the metal surface with the NIP carbonyl group. This could be attributed to either the reaction of the carbonyl oxygen with the metal via donation of electron pairs, or the complexation of the five-membered nitrogen with the metal. These findings suggest that there is a strong interaction between the NIP and the metal surface.

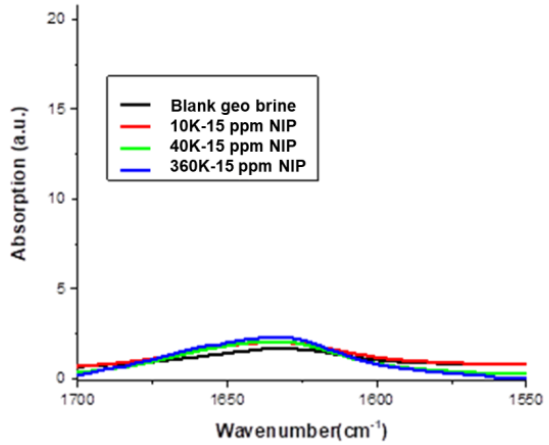

Figure 5: FT-IR spectra of increasing MW of NIP relating to its carboxyl group absorption at 1660 cm^{-1}.

3.3 Determining the effect of immersion time to the inhibition efficiency of varying concentration of 360K NIP

To further investigate the effect of concentration to the inhibition efficiency of NIP at its optimum MW, carbon steel samples were immersed in 5, 10,and 15 ppm NIP for 2, 7, 14, 30, and 60 days. PPS measurements were conducted to determine corrosion rate. Results are shown in Figure 6.

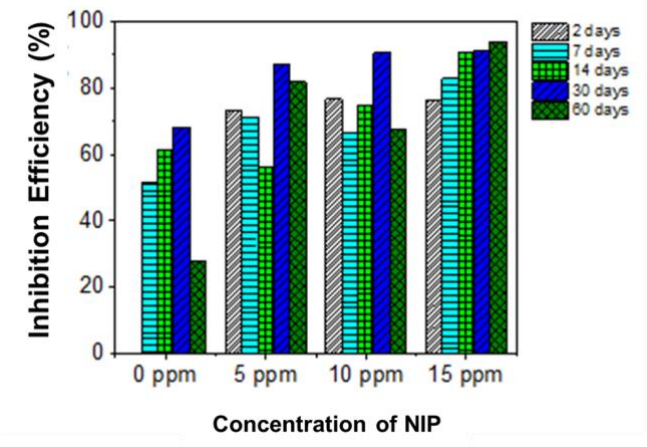

Figure 6: Inhibition efficiency of varying concentration of NIP in geothermal brine with respect to immersion time.

In addition, weight loss analysis was also used to determine corrosion rates of different concentrations. It is the simplest, and longest-established, method of estimating corrosion losses in plant and equipment. A weighed sample of the metal or alloy under consideration is introduced into the process, and later removed after a reasonable time interval, which for this study is 14 and 30 days. The coupon is then cleaned of all corrosion product and is reweighed. The weight loss is converted to a corrosion rate (CR) in mm/yr.

$$CR = \frac{m_2 - m_1}{A \times t \times \rho} \quad (2)$$

Where m_1 and m_2 are the weight (mg) of carbon steel after and before immersion, respectively. A is the surface area of the metal specimen (mm), t is the duration of immersion (yr), and ρ is the density of the material (mg/mm^3).

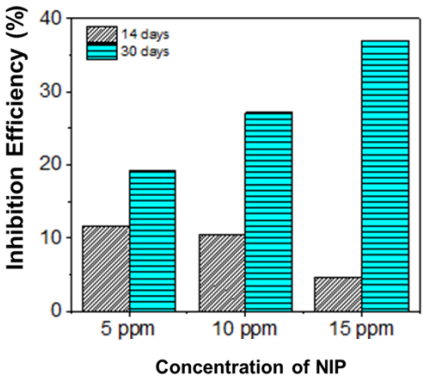

Figure 7: Inhibition Efficiency of CS immersed in varying concentration of NIP for 14 and 30 days.

Results of the weight loss analysis in Figure 7 generally show a lower protection efficiency as compared to the results obtained from the immersion studies. This is due to the fact that the corrosion rates of the samples have infinitesimal difference due to a short time of immersion. To be able to get a representative measurement of the actual corrosion rate in real systems, the duration of weight loss analysis should be set longer. However, the results of the 30 day immersion show similar trend on the effect of the concentration of NIP to the protection efficiency obtained using the electrochemical analysis.

The increasing trend of inhibition efficiency is attributed to the gradual formation of a passive film of silica. In low pH conditions, silica kinetics are slow, since at this condition it favors to be dispersed in solution in its monomeric form, $Si(OH)_4$, as reported by Iler (1979). For it to be precipitated out of the solution, it needs to react to the surface. $Si(OH)_4$ can condense with any pre-existing solid surface that bears OH groups with which it can react, like SiOH, or any MOH surface where M is a metal that will form a silicate. In actual industrial systems, silica has never been found to precipitate on clean metal, but instead a corrosion-product is always required first for it to form. In this case, oxidation of metal and/or formation of NIP film on the metal should occur first before a silica film can be formed (Salehi et al., 2011). Another factor which may delay the formation of silica layer is that polymer units or particles formed at low pH bear no charge, and aggregation begins to occur soon after polymeric particles are formed, not only because of the lack of charge on the particles, but also because the particles are extremely small and cease to grow after they reach a diameter of 2-3 nm. Since the rate of aggregation depends mainly on the number of particles per unit volume and less on their size, aggregation occurs even at low silica concentrations. Once a receptive surface is covered the condensation of $Si(OH)_4$, further deposition is silica on silica, building up a film, as discussed by Hermannsson (1970).

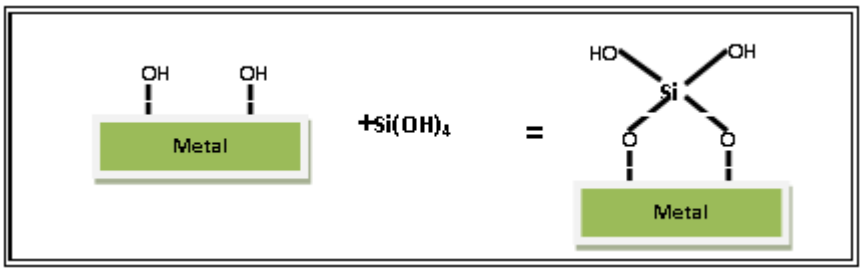

Figure 8: Deposition of monomeric silica at low pH on a solid surface.

For samples immersed for two weeks, a thin layer is formed. However, after two weeks, it was observed that there is a gradual build-up of the film. This was supported by the IR image taken of a samples immersed in blank brine solution and with NIP shown in Figure 9. Compared to the sample in geothermal brine alone, the sample immersed with NIP has almost uniform deposition on the surface. For coupons immersed in solution with NIP for one month, a two-layer film was observed where the top layer is flaky, loose and porous while the layer underneath it is compact and dense. This was also observed by Remoroza et al. (2010) on the coupons inserted in the production lines in Palinpinon which are exposed to low pH brine. It was observed that silica formation on carbon steel under acidic brine conditions yields corrosion films that consist of two layers of silica, a thin and dense basal layer that is attached to corrosion products and an overlying porous, thicker layer of globular silica dendrites.

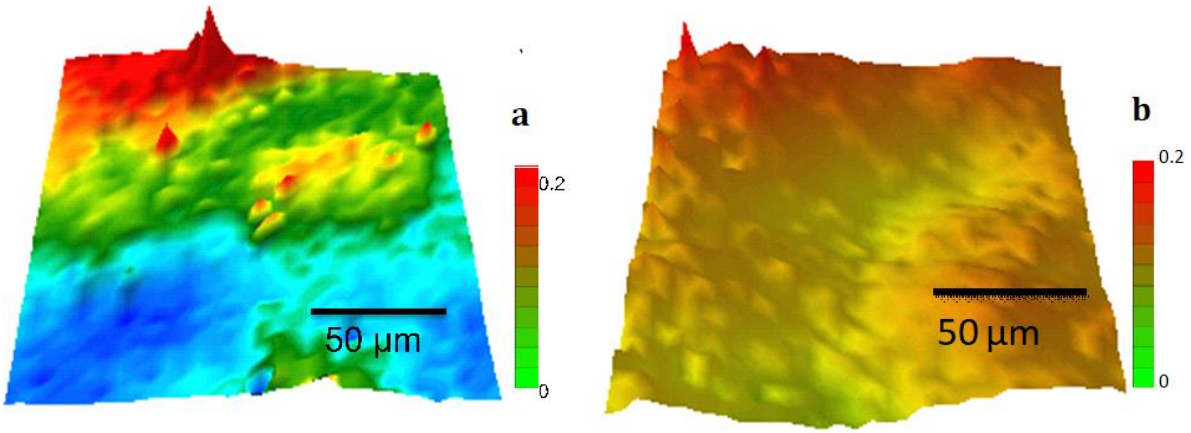

Figure 9: ATR IR image of carbon steel immersed in: a) synthetic geothermal brine; and, b) with PVP focused at wavenumber 1065 (Si-O).

This was also observed by the studies conducted by Lehrman and Shuldener (1952). They showed that the coatings formed on the metal mainly consist of metal oxide and silica. The formation of the film in dilute silica solution is dependent on the presence of small quantities of corrosion products on the metal surface. They also examined the films produced over time and microscopically showed that there are two layers present, with silica as the major component of the top layer exposed to the aqueous medium. When the hydrous metallic oxide film has been covered with a silica layer, further deposition is stopped, which accounts for the observed fact that prolonged exposure to silicate solutions does not build up thick films and that the thin films, when mechanically damaged, are self-healing. The attraction of positively charged corrosion products and negatively charged silica is therefore assumed to be part of the mechanism. The same observation was made by Demadis et al. (2004) on their study of the inhibition and growth control of colloidal silica in water treatment industry. Pronounced silica deposition phenomena was observed on metallic surfaces that is affected by severe corrosion process as reported by Remoroza et al. (2008).

Optical and SEM images of carbon steel immersed for different durations support the premise of gradual build-up of silica as seen on Figure 10 and Figure 11.

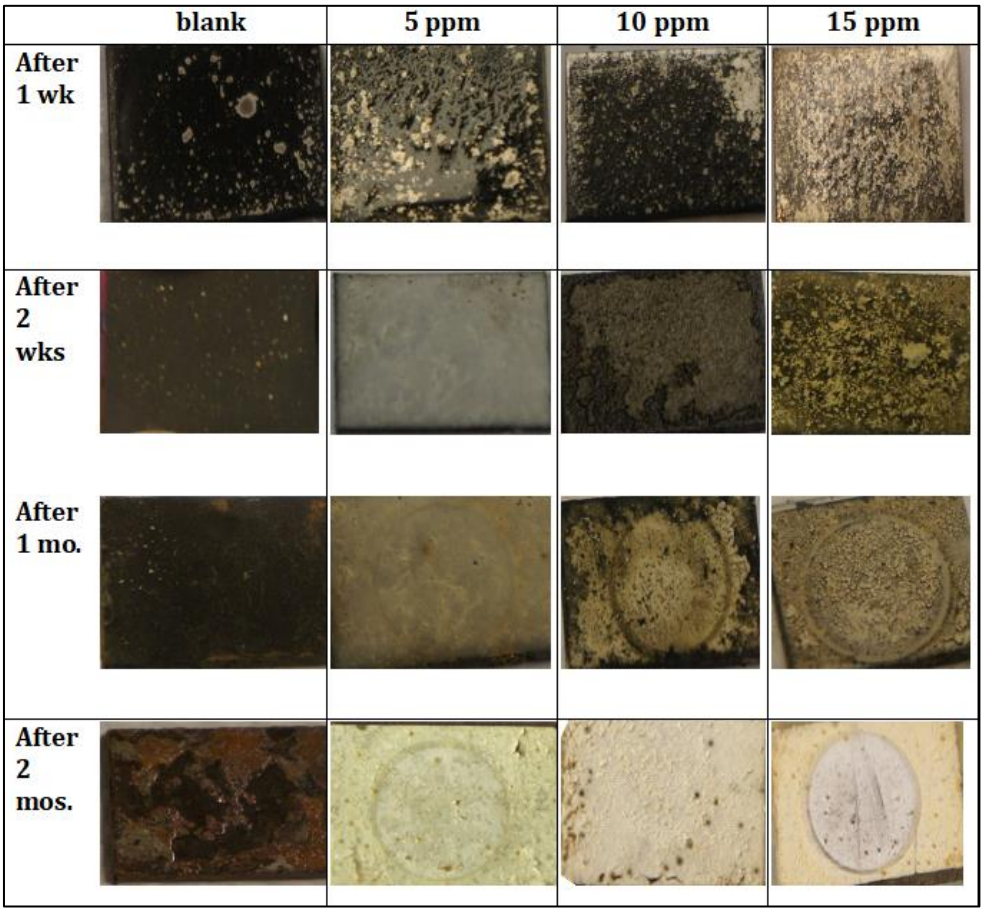

Figure 10: Optical images of carbon steel immersed in varying concentration of NIP in geothermal brine for different immersion durations.

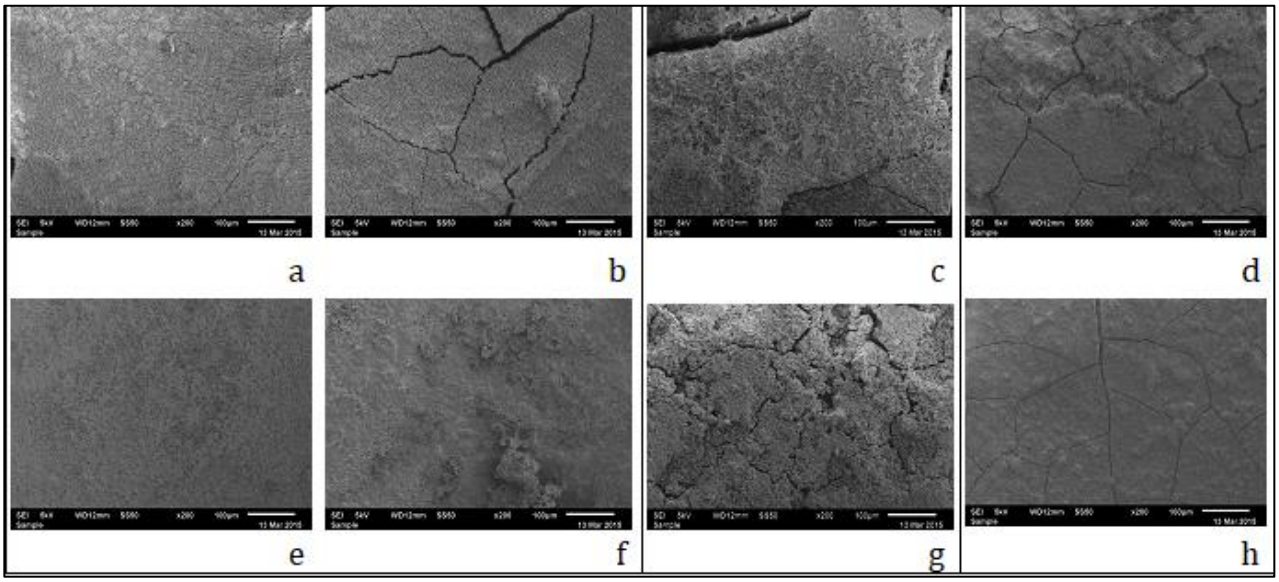

Figure 11: SEM images of carbon steel immersed for one month: a) top layer in blank geothermal brine; b) top layer in 5 ppm NIP; c) top layer in 10 ppm NIP; d) top layer in 15 ppm NIP; e) bottom layer in blank geothermal brine; f) bottom layer in 5 ppm NIP; g) bottom layer in 10 ppm NIP; and, h) bottom layer in 15 ppm NIP.

Based on the SEM images shown in Figure 11, for the top layer of CS samples immersed in varying concentration of NIP, there is no apparent change on the film formed. The top layer of all samples exhibit a compact film of silica. However, the surface of the bottom layer of these samples exhibit a significant change in terms of morphology and composition. Figure 11e shows the bottom layer of the carbon steel immersed in geothermal brine without NIP, where metal dissolution is evident and no film was observed. Unlike in the case of carbon steel samples immersed in geothermal brine with NIP, a passive film is still observable and as the concentration of NIP increases, the more compact the film appears to be.

Addition of NIP has a significant inhibition effect based on the EIS results gathered. EIS involves the application of a small sinusoidal perturbation to a sample under examination and the impedance modulus (z) is recorded as a function of the frequency (f). The analysis of the frequency behavior of the impedance allows the determination of the corrosion mechanism and the robustness of the passive film. To evaluate the performance of the passive film observed on the carbon steel, the impedance of the coating at the low frequency is observed. The higher the impedance at the low frequency region, the more effective the coating is. As the amount of NIP increases, the impedance value of the immersed CS also increases seen on Figure 12a. This is mainly due to the passive layers formed as seen on both the high and low frequency region.

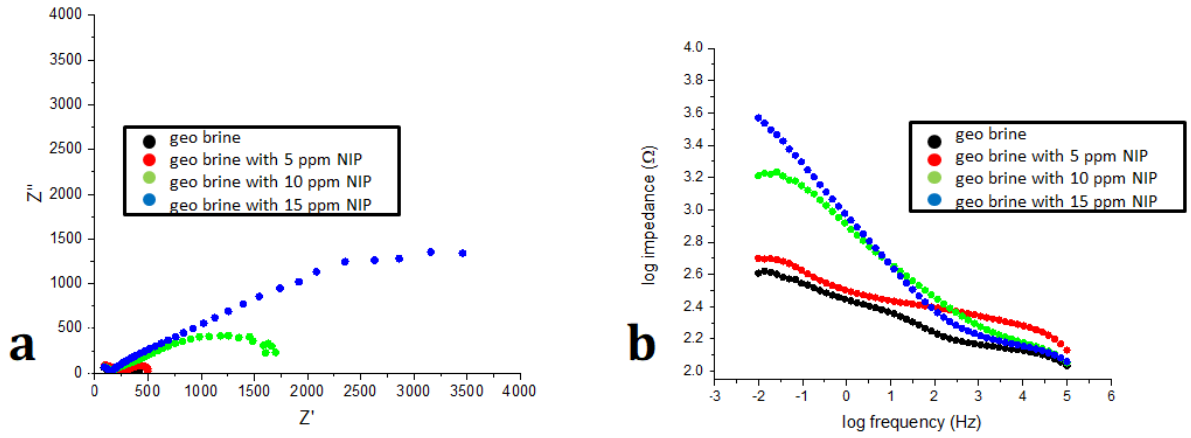

Figure 12: a) Nyquist plot; and, b) Bode plot of CS immersed in varying concentration of NIP for 1 month.

The integrity of the passive layer formed is supported by the Bode plot showing the significant difference of the passive film that was promoted by NIP as compared to the blank sample. The high inhibition efficiency of those immersed with NIP is due to the effectiveness of the passive layer formed in preventing the diffusion of corrosive species present in the acidic brine. To further investigate the formation of a 2-layer passive film, XPS analysis was conducted to determine the elemental composition of these two layers.

Results of XPS analysis of the film form in the bottom layer of CS in geothermal brine, shown in Table 1, alone has a significant percentage of iron which suggest that the layer is already on the metal surface. Also, the amount of silica is relatively low compared to that found in the film of CS under geothermal brine with NIP. On the other hand, the iron in the CS immersed in geothermal brine with NIP is lower, which suggest less metal oxidation. This further supports the results previously observed with the SEM and EIS analyses.

Table 1: XPS analysis of the bottom film formed in CS immersed in geothermal brine and in geothermal brine with 15 ppm NIP.

% elemental composition	CS in geothermal brine	CS in geothermal brine with 15 ppm PVP
O	56.9	60
Si	5.1	15.8
C	11.5	6.8
Fe	8.1	0.7
Cl	1.6	3
Ca	<0.1	<0.1
S	<0.1	<0.1
Mg	8.7	7.2
Na	8.3	6.7
K	<0.1	<0.1

3.4 Effect of temperature

The inhibition property of NIP in high temperature was also evaluated by comparing the instantaneous corrosion rates of coupons immersed in varying solutions of NIP at room and actual line process temperature (160°-180°C). The increase in the inhibition efficiency with the increase in temperature suggests that NIP is still thermally stable at high temperature and was able to adsorb on the metal surface. A physisorption mechanism was proposed by Umoren et al. (2008) by considering the fact that NIP could interact with the corroding metal surface via the protonated N atom, which can be adsorbed at cathodic sites and hinder the hydrogen evolution reaction, with possible contributions from the lone pair of electrons on the oxygen atom. This may be facilitated by the presence of the vacant d-orbitals of iron. The adsorption of NIP creates a barrier for mass and charge transfers.

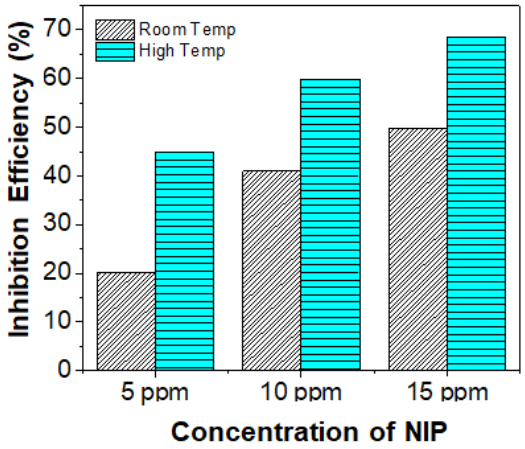

Figure 13: Inhibition efficiency of CS immersed in varying concentration of NIP at room and two-phase line temperature (180°C).

4. SUMMARY AND CONCLUSION

This study was able to determine the inhibitor concentration at which the NIP is soluble in the acidic geothermal fluid by a simple solubility technique using Tyndall effect. The corrosion rate of carbon steel in acidic geothermal fluid in the presence of varying molecular weight of polymeric inhibitor was determined and evaluated. For this study, inhibition efficiency increases as MW increases since it is only dependent on the surface area of the metal covered by the NIP. The real time change in the corrosion rate of carbon steel in acidic geothermal fluid in the presence of varying concentrations of the polymeric inhibitor was observed. The decrease in the corrosion rate as immersion time is prolonged is due to the gradual formation of a silica layer as promoted by the NIP formed on the metal surface. The effect of temperature on the corrosion rate of carbon steel in acidic geothermal fluid in the presence of varying concentrations of the polymeric inhibitor was also considered to determine the applicability of NIP in actual geothermal systems. Even at high temperature and pressurized conditions, NIP was still able to inhibit the corrosion process. An inhibition mechanism of NIP may be deduced based on the results of the tests conducted. NIP acts as a cathodic inhibitor by forming a strong interaction with the metal, thus forming a film. The polymer film formed acts as a seeding site for the silicic acid dispersed in the acidic geothermal brine to polymerize by binding to the carbonyl oxygen of NIP.

Despite the satisfactory results obtained from the study conducted, it is still recommended to extend the study to dynamic conditions to simulate the actual line condition. Kinetics play a major role in various processes in the geothermal industry. It could have a significant effect on the inhibition and protection efficiencies of the tested polymeric materials.

REFERENCES

Al Juhaiman, L., Mustafa, A., & Mekhamer, W:. Int.J.Electrochem.Sci.,7, (2012), 8578-8596.

Antonijevic, M., & Petrovi, M: Int.J.Electrochem.Sci , 1, (2008).

Arthur, D., Jonathan, A., Ameh, P., & Anya, C: A review on the assessment of polymeric materials used as corrosion inhibitor if metals and alloys. International Journal of Industrial Chemistry, (2013), 1-9.

Casper, L.A. and Pinchback, T.R: Geothermal scaling and corrosion: Philadelphia, American Society for Testing and Materials, 262 p. (ASTM, 1916 Race St., Philadelphia, PA 19103 (1980).

Daouadji, M. M., & Chelali, N: Influence of Molecular weight of Poly(otho-ethoxyaniline) on the corrosion inhibition efficiency of mild steel in acidic media. Journal of Applied Polymer Science, 9, (2003), 1275-1284.

Demadis, K., & Neofotistiu, E: Inhibition and Growth Control of Colloidal Silica: Designed Chemical Approaches. Materials Performance, (2004), 38-41.

El-Maksuod, S: Int.J.Electrochem.Sci, 3, (2008), 275.

Emamgholizadeha, A., Rostamia, A., Omrania, A., & Rostamib, A: Performance of EP/PpPDA and EP/PpPDA/SiO2 nanocomposite on corrosion inhibition of steel in hydrochloric acid solution. Progress in organic Coatings, 82, (2015), 7-16.

Finsgar, M., & Jackson, J: Application of corrosion inhibitors for steels in acidic media for the oil and gas industry: A review. Corr.Sci. , 86, (2014), 17-41.

Gill, J. Scale Control in Geothermal Brines. Transactions of Geothermal Resources Council 2008 Annual meeting, (2008).

Graf, C., Vossen, D., Imhof, A., & van Blaaderen, A: A general method to coat colloidal particles with silica. Langmuir, 19, (2003), 6693-6700.

Gu, T., Liu, X., Chai, W., Li, B., & Sun, H: A preliminary research on polyvinyl alcohol hydrogel: A slowly-released anti-corrosion and scale inhibitor. Journal of Petroleum Science and Engineering, 122, (2015), 453-457.

Hermannsson, S: Corrosion of Metals and the Forming of a Protective Coating on the Inside of Pipes Carrying Thermal Waters Used by the Reykjavik Municipal Distrcit Heating Service. Geothermics, 2, (1970), 1602-1612.

Hermannsson, S: Corrosion of Metals and the Forming of a Protective Coating on the Inside of Pipes Carrying Thermal Waters Used by the Reykjavik Municipal Distrcit Heating Service. Geothermics, 2, (1970), 1602-1612.

Iler, R: The Chemistry of Silica; Solubility, Polymerization, Colloid and Surface Properties and Biochemistry of Silica. John Wiley & Sons (1979).

Jing, C., & Hou, J: Sol-Gel derived Alumina/NIP hybrid nanocomposite film on metal for corrosion resistance. Journal of Apllied Polymer Science, 105, (2007), 697-705.

Jordan, O., Borromeo, C., Reyes, R., & Ferrolino, S: A Technical and Cost Assessment of Silica deposition in the Palinpinon-I geothermal field, Philippines, over 16 years of production and reinjection. World Geothermal Congress. Kyushu-Tohoku, Japan (2000).

Khelifa, F., Druart, M., Habibi, Y., Benard, F., Leclere, P., Olivier, M., et al: Sol-gel incorporation of silica nanofillers for tuning the anti-corrosion protection of acrylate-based coatings. Progress in Organic Coatings, 76, (2013), 900-911.

Kim, H., & Hwang, T: Corrosion protection enhancement effect by mixed silica nanoparticles of different sizes incorporated in a sol-gel silica film. . J Sol-Gel Sci Technol, 63, (2012), 563-568.

Kumaraguru, S., Veeraraghavan, B., & Popov, B: Development of an Electroless Method to Deposit Corrosion-Resistant Silicate Layers on Metallic Substrates. Journal of the Electrochemical Society, 153, (2006), 253-259.

Lehrman, L., & Shuldener, H: Action of sodium silicate as a corrosion inhibitor in water piping. Industrial and Engineering Chemistry, 44(8), (1952), 1765- 1769.

Lopez, A., Urena, A., & Rams, J: Surface Coating Technology, 203, (2009), 1474-1480.

Manimaran, N., Rajendran, S., Manivanan, M., & John Mary, S: Corrosion Inhibition of Carbon Steel By polyacrylamide. Res.J.Chem.Sci , 2(3), (2012), 52-57.

Mundhenk, H., Sanjua, B., Kohl, S., & Zorn, R: Corrosion and scaling as interrelated phenomena in an operating geothermal power plant. Corrosion Science, (2013), 17-28.

Pech, D., Steyer, P., & Millet, J: Corrosion Science, 50, (2008), 1492-1497.

Remoroza, A., Doroodchi, E., & Moghtaderi, B: Corrosion Inhibition of Acid-Treated Geothermal Brine- results from Pilot Testing in Southern Negros, Philippines. World Geothermal Congress 2010. Bali, Indonesia (2010).

Remoroza, A., Mejorada, A., & Salazar, A: Field Testing of pH Modification Silica Inhibition with Chemical Corrosion Inhibition. Thiry-Third Workshop on Geothermal Reservoir Engineering. Stanford, California (2008).

Salehi, M., Nasr-Esfahani, M., Sharifian-Esfahani, A., & Ekramian, E: Magnetite/Polyvinylpyrrolidone Nanocomposite: Green Simple Fabrication and Characterization. 2nd International Conference on Chemistry and Chemical Engineering (pp. 174-177). Singapore (2011).

See, F. S: Silica Inhibitor Hot Injection Test at Bacman Geothermal Production Field, Botong, Philippines. World Geothermal Congress. Bali, Indonesia (2010).

Spinthaki, A., Stathoulopoulou, A., & Demadis, K.: The interplay between cationic polyethyleneimine and anionic polyelectrolytes for the control of silica scale formation in process waters. International Journal of Corrosion and Scale Inhibition, 2, (2015), 125-138.

Thomas, G: Some new fundamental aspects in corrosion inhibition. 5th Euro. SYmp. Corr. Inhibitors, (p. 453). Ferrara, Italy (1981).

Umoren, S., Ogbobe, O., Igwe, I., & Ebenso, E: Inhibition of Mild steel corrosion in acidic medium using synthetic and naturally occuring polymers and synergistic halide additives. Corr.Sci.,50, (2008), 7.

Zheludkevich, Sachukin, & Yasakav: Anticorrosion coatings with self-healing effect based on Nanocontainers impregnated with corrosion inhibitor. Chemistry of materials, 3, (2007), 402-411.